



Two-loop heavy-top effects in the Standard Model

Riccardo Barbieri^{1, 2, 3}, Matteo Beccaria^{1, 2}, Paolo Ciafaloni^{1, 2}
Giuseppe Curci^{2, 1} and Andrea Viceré^{4, 2}

Abstract

We give a detailed description of the calculation in the Standard Model of all the m_t^4 radiative correction effects to the electroweak precision observables for arbitrary values of the Higgs mass.

1 Introduction

In the analysis of the electroweak precision data, the significance of virtual top effects is well known. On one side, they allow the extraction of relevant indirect information on the top mass; on the other side, at least until the top quark mass itself will be directly measured, they mask other perhaps more significant effects. With these general motivations in mind, we have made a calculation in the Standard Model (SM) of all the radiative correction effects to the electroweak precision tests that scale like the fourth power of the top Yukawa coupling g_t . This amounts to extending to two loops, for arbitrary values of the Higgs mass, the original calculations of the one-loop contributions, growing like m_t^2 , to the electroweak ρ parameter [1] and the GIM-violating $Zb\bar{b}$ vertex [2]. To our knowledge, such calculation has previously been made for ρ , but not for the $Zb\bar{b}$ vertex, and only in the limiting case of a Higgs mass m_H negligible with respect to m_t [3]. A preliminary account of the results was given in [4] in the asymptotic regime $m_H/m_t \gg 1$. Here we intend to give a description of the calculation and of the complete results for arbitrary values of m_H/m_t .

At least from a technical point of view, a rather interesting aspect of these m_t corrections to the electroweak precision observables is that they have little to do with the gauge structure of the SM, since they are present even for vanishing gauge couplings. On the contrary, they only arise from the symmetry-breaking sector of the theory restricted to the scalar self-interactions and to the top Yukawa coupling.

How to exploit these properties to simplify the actual calculation in a significant way has already been described in [4]: from the Ward identities of the SM Lagrangian with the gauge interactions switched off, it is immediate to relate the physical quantities to appropriate renormalization constants of this reduced Lagrangian. These renormalization constants are the quantities that have to be computed.

In section 2 we write the Lagrangian, we define the physical parameters as well as the relevant renormalization constants and we recall their relationships. In section 3 we give details of the calculation of the regularized, unrenormalized quantities. To allow a comparison, since the full expressions for arbitrary values of the ratio m_t/m_H are too long to be written explicitly, we give analytic expansions of the different results for $m_t/m_H \ll 1$ and $m_t/m_H \gg 1$. In section 4 we describe our renormalization procedure. Finally our overall analytic and numerical results are given in section 5, together with the physical conclusions.

In Appendix A we derive the Ward identities necessary to relate the different physical quantities to the appropriate renormalization constants. In Appendix B we address the question of the regularization procedure.

2 Lagrangian and reference formulae

Our reference Lagrangian, involving the Higgs doublet Φ , the third-generation left-handed quark doublet $Q_L = (t_L, b_L)$ and the right-handed top-quark field t_R , is

$$L = |\partial_\mu \Phi|^2 + i\bar{t}\not{\partial}t + i\bar{b}\not{\partial}b - \mu^2 |\Phi|^2 - \lambda |\Phi|^4 + g_L \bar{Q}_L \not{t}_R \Phi + g_t \bar{t}_R Q_L \Phi^* \quad (1)$$

Since we are neglecting the bottom Yukawa coupling, b_R is a non-interacting field. Shifting the Φ field in the usual way to

$$\Phi = \begin{pmatrix} v + \frac{1}{\sqrt{2}}(H + i\chi) \\ i\varphi^- \end{pmatrix}, \quad (2)$$

one obtains a considerably longer expression

$$\begin{aligned} L &= L_{Kinetic} + L_{Yukawa} + L_{Scalar\ Potential} \\ L_{Kinetic} &= i\bar{t}\not{\partial}t + i\bar{b}\not{\partial}b + \partial_\mu\varphi^+\partial_\mu\varphi^- + \frac{1}{2}(\partial_\mu\chi)^2 + \frac{1}{2}(\partial_\mu H)^2 \\ L_{Yukawa} &= g\left(v\bar{t}t + \frac{1}{\sqrt{2}}\bar{t}tH + \frac{i}{\sqrt{2}}\bar{t}\gamma_5 t\chi + i\bar{b}_L t_R\varphi^- - i\bar{t}_R b_L\varphi^+\right) \\ L_{Scalar\ Potential} &= -\sqrt{2}v(\mu^2 + 2\lambda v^2)H - \frac{1}{2}(\mu^2 + 6\lambda v^2)H^2 \\ &\quad - (\mu^2 + 2\lambda v^2)\left(\frac{1}{2}\chi^2 + \varphi^+\varphi^-\right) - \sqrt{2}\lambda v(H^3 + H\chi^2 + 2H\varphi^+\varphi^-) \\ &\quad - \lambda\left(\frac{1}{4}(H^4 + \chi^4) + \frac{1}{2}H^2\chi^2 + (\varphi^+\varphi^-)^2 + \varphi^+\varphi^-(\chi^2 + H^2)\right) \end{aligned} \quad (3)$$

involving the physical Higgs field H and the charged and neutral Goldstone bosons φ, χ respectively. Other than the original parameters g, μ, λ , the Lagrangian (3) contains the vacuum expectation value v as well. A relation between v, g, μ, λ arises from the requirement of the vanishing of the Goldstone boson masses and of the tadpole terms. Since λ and μ only enter at the two-loop level in the calculation, in practice we can proceed as follows: we enforce by hand the vanishing of the Goldstone masses and of the tadpoles, we treat v as a free parameter and, at the end, we eliminate μ by the tree-level relation $\mu^2 + 2\lambda v^2 = 0$. Using the Lagrangian (3), the constants that we need to compute are defined by $(P_{L,R} = 1/2(1 \mp \gamma_5))$:

$$\begin{aligned} \Gamma(p, p') &\simeq Z_1^{\not{p} - \not{p}'} P_L \text{ at } p \simeq p' \\ \frac{\partial\Pi(q^2)}{\partial q^2}\Big|_{q^2=0} &= (Z_2^\chi - 1) \quad , \quad \frac{\partial\Pi^\pm(q^2)}{\partial q^2}\Big|_{q^2=0} = (Z_2^\pm - 1) \end{aligned} \quad (4)$$

$$S_b^{-1}(p) \simeq iZ_2^b p P_L + i\bar{p} P_R \text{ at } p^2 \simeq 0$$

in terms of the irreducible vertex $\Gamma(p, p')$ between b quarks of momentum p, p' and the neutral Goldstone boson χ , the self energies $\Pi(q), \Pi^\pm(q)$ of the neutral and charged Goldstone bosons and the b -quark propagator $S_b(p)$. As we explain in Appendix A, the Ward identities of the (spontaneously broken) global symmetries of the Lagrangian (1) allow us to express the electroweak ρ parameter and the GIM-violating $Z \rightarrow b\bar{b}$ vertex τ in terms of these constants. We define ρ and τ from the Z widths into $\mu^+\mu^-$ and $b\bar{b}$ via

$$\begin{aligned} \Gamma(Z \rightarrow \mu^+\mu^-) &= \frac{G_\mu M_Z^2}{8\pi\sqrt{2}} (g_{\mu\nu}^2 + g_{\mu A}^2) \\ \Gamma(Z \rightarrow b\bar{b}) &= \frac{G_\mu M_Z^2}{8\pi\sqrt{2}} \left[\sqrt{1 - \frac{4m_b^2}{M_Z^2}} \left(g_{bB}^2 + g_{bA}^2 \right) \left(1 + 2\frac{m_b^2}{M_Z^2} \right) - 6g_{bA}^2 \frac{m_b^2}{M_Z^2} \right] \end{aligned} \quad (5)$$

$$g_{\mu\nu} = 1 - 4s^2 \quad , \quad g_{\mu A} = 1 \quad (6)$$

$$g_{bV} = 1 - \frac{4}{3}s^2 + \tau \quad , \quad g_{bA} = 1 + \tau$$

and

$$s^2 = \frac{1}{2} \left(1 - \sqrt{1 - \frac{4\pi\alpha}{\sqrt{2}G_\mu M_Z^2 \rho}} \right). \quad (7)$$

The reference formulae are then [4]

$$\rho = \frac{Z_2^\rho}{Z_2^\chi} \quad , \quad \tau = \frac{Z_1^\chi}{Z_2^\rho}. \quad (8)$$

These are exact expressions, valid to all orders.

For a two-loop calculation, it is useful (and customary) to rewrite ρ as

$$\frac{1}{\rho} = 1 + \frac{Z_2^\chi - Z_2^\rho}{Z_2^\rho}, \quad (9)$$

which makes it clear that, since the expansion of Z_2^ρ starts from 1, only the difference between the two wave-function renormalization constants $Z_2^\chi - Z_2^\rho$ must be computed up to two-loop order. We can therefore discard all the single graphs, which do not contribute to this difference.

3 Explicit calculation of the regularized quantities

The diagrams that are relevant to compute ρ and τ to order g_t^2 are shown in Fig. 1 (diagrams with pure scalar loops in the Goldstone boson self energies do not contribute to the difference $Z_2^\rho - Z_2^\chi$, but the full $Z_2^{\rho(\varphi)}$ expression at one loop is needed for evaluating ρ at \hbar^2 order). In the following we shall express the renormalization factors as sums over the contributions coming from the different graphs

$$\begin{aligned} Z_1^\chi &= \sum_t \delta Z_1^{\chi(t)} \\ Z_2^\chi &= 1 + \sum_t \delta Z_2^{\chi(t)} \\ Z_2^\rho &= 1 + \sum_t \delta Z_2^{\rho(t)}. \end{aligned} \quad (10)$$

Although the vertex diagram of Fig. 1a is divergent by power counting, its contribution to the Z_1^χ constant is finite:

$$\delta Z_1^{\chi(1a)} = -\frac{g_t^2}{(4\pi)^2}. \quad (11)$$

The self energy diagrams 1b and c give separate logarithmically divergent contributions to the Goldstone boson self energy renormalization constants. Here and throughout the

paper we use the dimensional regularization with an anticommuting γ_5 matrix (the so-called Naive Dimensional Regularization, NDR). We illustrate in Appendix B why, for the purposes of the present calculation, this regularization scheme, while preserving the correct chiral Ward identities, does not lead to any inconsistency related to the chiral anomaly. From the diagrams of Fig. 1b and c we obtain

$$\delta Z_2^{(1b)} = \frac{1}{(4\pi)^2} \left\{ -\frac{2v^2\lambda^2}{\mu^2} + g_t^2 N_c \left[\frac{1}{2} + \frac{1}{\varepsilon} - \gamma_E - \log \frac{m_t^2}{4\pi\mu^2} \right] \right\} \quad (12)$$

$$\delta Z_2^{(1c)} = \frac{1}{(4\pi)^2} \left\{ -\frac{2v^2\lambda^2}{\mu^2} + g_t^2 N_c \left[\frac{1}{\varepsilon} - \gamma_E - \log \frac{m_t^2}{4\pi\mu^2} \right] \right\}$$

where $\varepsilon = 2 - d/2$.

Using the lowest-order relation

$$g_t^2 = \frac{m_t^2}{v^2} = \frac{4}{\sqrt{2}} G_\mu m_t^2, \quad (13)$$

eqs. (11) and (13) are enough to get the one-loop corrections [1, 2]

$$\rho = 1 + N_c \frac{G_\mu m_t^2}{8\pi^2 \sqrt{2}} \quad (14)$$

$$\tau = -\frac{G_\mu m_t^2}{4\pi^2 \sqrt{2}}.$$

Notice that at this order, since Z_1^χ starts from g_t^2 , there is no need to compute the b wave-function renormalization constant, which starts from 1.

The relevant two-loop diagrams contributing to the vertex constant Z_1^χ are shown in Fig. 2. All the diagrams are finite, except for the divergent one-loop self energy insertions in Fig. 2e and 2f. Except for diagram 2b, which does not involve Higgs internal lines, all other (sets of) diagrams give contributions, that are functions of the ratio $r \equiv (m_t/m_H)^2$, with quite involved explicit expressions. Making reference to section 5 for complete numerical values, we give in the following the leading terms in an asymptotic expansion as $r \rightarrow 0$ and $r \rightarrow \infty$. We have, for $r \ll 1$, omitted terms $O(r \log^2 r)$,

$$\begin{aligned} \delta Z_1^{\chi(2a)} &= \frac{g_t^4}{(4\pi)^4} \left[-\frac{1}{16} - \frac{3}{8} \log r \right] \\ \delta Z_1^{\chi(2b)} &= \frac{g_t^4}{(4\pi)^4} \frac{N_c}{2} \\ \delta Z_1^{\chi(2c)} &= \frac{g_t^4}{(4\pi)^4} \left[-\frac{27}{32} + \frac{\pi^2}{12} + \frac{11}{16} \log r + \frac{1}{16} \log^2 r \right] \\ \delta Z_1^{\chi(2d)} &= \frac{g_t^4}{(4\pi)^4} \left[\frac{1}{16} - \frac{\pi^2}{12} + \frac{7}{8} \log r - \frac{1}{4} \log^2 r \right] \\ \delta Z_1^{\chi(2e)} &= \frac{g_t^4}{(4\pi)^4} \left[N_c \left(\frac{1}{\varepsilon} - 2\gamma_E - 2 \log \frac{m_t^2}{4\pi\mu^2} + 1 + \frac{1}{12} \log r \right) + \frac{1}{4r} + \frac{1}{72} \right] \end{aligned}$$

$$\begin{aligned} \delta Z_1^{\chi(2f)} &= \frac{g_t^4}{(4\pi)^4} \left[\frac{1}{\varepsilon} - 2\gamma_E - 2 \log \frac{m_t^2}{4\pi\mu^2} + \frac{1}{2} - \frac{\pi^2}{24} - \frac{1}{4} \log r \right] \\ \delta Z_1^{\chi(2g)} &= \frac{g_t^4}{(4\pi)^4} \left[-\frac{1}{4} - \frac{\pi^2}{24} - \frac{1}{2} \log r \right]. \end{aligned} \quad (15)$$

A few comments are in order on the results for large Higgs masses. In the $r \rightarrow 0$ limit only the contribution from Fig. 2e has a term divergent as $1/r$. Taking into account the g_t^4 factor in front and that, to leading order, $1/r = 4/g_t^2$, such term is actually of the form $g_t^2 \lambda$ and grows like $m_t^2 m_H^2$. As we shall see, however, such terms get absorbed by the renormalization procedure, with the overall net result that the two-loop corrections grow at most as $\log^2 m_H^2$ for large m_H . Also the separate diagrams in 2a give individual contributions growing like m_H^2 (or λ), but cancelling one each other. This is related to the softer high-energy behaviour of the amplitude $\varphi^+ \varphi^- \rightarrow \chi \chi$ when the two sub-diagrams in 2a contributing to this amplitude are summed together.

Analogously, for $r \gg 1$ and omitting terms $o\left(\frac{1}{r}\right)$ we have

$$\begin{aligned} \delta Z_1^{\chi(2a)} &= \frac{g_t^4}{(4\pi)^4} \left[\frac{1}{24r} (3 + \pi^2) \right] \\ \delta Z_1^{\chi(2b)} &= \frac{g_t^4}{(4\pi)^4} \frac{N_c}{2} \\ \delta Z_1^{\chi(2c)} &= \frac{g_t^4}{(4\pi)^4} \left[\frac{1}{6r} (\pi^2 - 12 - 3 \log r) \right] \\ \delta Z_1^{\chi(2d)} &= \frac{g_t^4}{(4\pi)^4} \left[\frac{1}{24r} (9 - 7\pi^2) \right] \\ \delta Z_1^{\chi(2e)} &= \frac{g_t^4}{(4\pi)^4} N_c \left(\frac{1}{\varepsilon} - 2\gamma_E - 2 \log \frac{m_t^2}{4\pi\mu^2} + 1 \right) \\ \delta Z_1^{\chi(2f)} &= \frac{g_t^4}{(4\pi)^4} \left[\frac{1}{\varepsilon} - 2\gamma_E - 2 \log \frac{m_t^2}{4\pi\mu^2} - \frac{13}{4} + \frac{\pi^2}{3} + \frac{1}{24r} (139 - 14\pi^2 + 6 \log r) \right] \\ \delta Z_1^{\chi(2g)} &= \frac{g_t^4}{(4\pi)^4} \left[\frac{3}{2} - \frac{\pi^2}{6} + \frac{1}{24r} (\pi^2 - 7 + 6 \log r) \right]. \end{aligned} \quad (16)$$

Both eqs. (15) and (16) correspond to regularized unsubtracted expressions. The only renormalization condition that we imposed is the vanishing of the renormalized mass of the internal χ , φ and b propagators.

The overall results for the regularized vertex constant Z_1^χ in the two asymptotic regimes are given by

$$\begin{aligned} \delta Z_1^\chi|_{r \ll 1} &= \frac{g_t^4}{(4\pi)^4} \left[(N_c + 1) \left(\frac{1}{\varepsilon} - 2\gamma_E - 2 \log \frac{m_t^2}{4\pi\mu^2} \right) + \frac{3N_c}{2} - \frac{167}{288} - \frac{\pi^2}{12} + \frac{25}{48} \log r - \frac{5}{16} \log^2 r \right] \\ \delta Z_1^\chi|_{r \gg 1} &= \frac{g_t^4}{(4\pi)^4} \left[(N_c + 1) \left(\frac{1}{\varepsilon} - 2\gamma_E - 2 \log \frac{m_t^2}{4\pi\mu^2} \right) + \frac{3N_c}{2} + \frac{\pi^2}{6} - \frac{7}{4} - \frac{5}{8r} (\pi^2 - 6) \right]. \end{aligned} \quad (17)$$

According to eq. (8) the calculation of the full g_t^4 correction to τ also requires the one-loop expression for the b wave-function renormalization constant. From the diagram of Fig. 3 we get

$$Z_2^b = 1 + \frac{g_t^2}{(4\pi)^2} \left[2 \left(\varepsilon - \gamma_E - \log \frac{m_t^2}{4\pi\mu^2} \right) + \frac{3}{4} \right]. \quad (18)$$

The two-loop diagrams contributing to the difference $(Z_2^b - Z_2^{\tilde{\chi}})$ of the Goldstone boson wave-function renormalization constants are shown in Fig. 4. The diagram of Fig. 4a for $Z_2^{\tilde{\chi}}$ has no counterpart for Z_2^b . As before we give the separate contributions to $(Z_2^b - Z_2^{\tilde{\chi}})$ from the individual sets of diagrams, for $r \rightarrow 0$ and $r \rightarrow \infty$.

For $r \ll 1$, and omitting $O(r \log^2 r)$ terms, one has

$$\begin{aligned} (Z_2^b - Z_2^{\tilde{\chi}})^{4a} &= \frac{g_t^4}{(4\pi)^4} N_c \left[-\frac{1}{2} + \frac{\pi^2}{6} + \frac{1}{2} \log r + \frac{1}{2} \log^2 r \right] \\ (Z_2^b - Z_2^{\tilde{\chi}})^{4b} &= \frac{g_t^4}{(4\pi)^4} N_c \left[-\frac{3}{4\varepsilon} + \frac{3}{2} \gamma_E + \frac{3}{2} \log \frac{m_t^2}{4\pi\mu^2} \right. \\ &\quad \left. + \frac{25}{16} - \frac{\pi^2}{4} + \frac{1}{8} \log r - \frac{1}{8} \log^2 r \right] \\ (Z_2^b - Z_2^{\tilde{\chi}})^{4c} &= \frac{g_t^4}{(4\pi)^4} N_c \left[\frac{3}{2} + \frac{\pi^2}{6} + \log r \right] \\ (Z_2^b - Z_2^{\tilde{\chi}})^{4d} &= \frac{g_t^4}{(4\pi)^4} N_c \left[\frac{\pi^2}{6} + \log r \right]. \end{aligned} \quad (19)$$

For $r \gg 1$, and omitting $o\left(\frac{1}{r}\right)$ terms,

$$\begin{aligned} (Z_2^b - Z_2^{\tilde{\chi}})^{4a} &= \frac{g_t^4}{(4\pi)^4} N_c \left[-2 + \frac{11}{12r} + \frac{1}{2r} \log r \right] \\ (Z_2^b - Z_2^{\tilde{\chi}})^{4b} &= \frac{g_t^4}{(4\pi)^4} N_c \left[\frac{3}{4\varepsilon} + \frac{3}{2} \gamma_E + \frac{3}{2} \log \frac{m_t^2}{4\pi\mu^2} \right. \\ &\quad \left. + \frac{41}{8} - \frac{\pi^2}{2} - \frac{1}{6r} (31 - 3\pi^2 + 3 \log r) \right] \\ (Z_2^b - Z_2^{\tilde{\chi}})^{4c} &= \frac{g_t^4}{(4\pi)^4} N_c \left[-\frac{1}{8r} \right] \\ (Z_2^b - Z_2^{\tilde{\chi}})^{4d} &= \frac{g_t^4}{(4\pi)^4} N_c \left[-\frac{1}{2r} \right]. \end{aligned} \quad (20)$$

Only the set of diagrams 4b contains a divergent term. In fact the various individual diagrams contributing to this set also show double-pole terms, $1/\varepsilon^2$, as $\varepsilon \rightarrow 0$, that cancel in the sum. The overall results in the two asymptotic regimes are

$$(Z_2^b - Z_2^{\tilde{\chi}})^{4e} \Big|_{r \ll 1} = \frac{g_t^4}{(4\pi)^4} N_c \left[\frac{3}{4} \left(\frac{1}{\varepsilon} - 2\gamma_E - 2 \log \frac{m_t^2}{4\pi\mu^2} \right) + \frac{41}{16} + \frac{\pi^2}{4} + \frac{3}{8} (7 \log r + \log^2 r) \right]$$

(21)

$$(Z_2^b - Z_2^{\tilde{\chi}})^{4e} \Big|_{r \gg 1} = \frac{g_t^4}{(4\pi)^4} N_c \left[-\frac{3}{4} \left(\frac{1}{\varepsilon} - 2\gamma_E - 2 \log \frac{m_t^2}{4\pi\mu^2} \right) + \frac{25}{8} - \frac{\pi^2}{2} + \frac{1}{8r} (4\pi^2 - 39) \right].$$

4 Renormalization

The regularized expressions for ρ and τ obtained in the previous section have the form

$$\frac{1}{\rho} = 1 - N_c y \left(\rho_{\text{reg}}^{(1)} + y \rho_{\text{reg}}^{(2)} \right) \quad (22)$$

$$\tau = -2y \left(\tau_{\text{reg}}^{(1)} + y \tau_{\text{reg}}^{(2)} \right),$$

where

$$y = \frac{g_t^2}{32\pi^2}$$

and

$$\begin{aligned} \rho_{\text{reg}}^{(1)} &= 1 + \frac{\varepsilon}{2} - \varepsilon \log \frac{m_t^2}{4\pi\mu^2} - \varepsilon \gamma_E + \mathcal{O}(\varepsilon^2) \\ \tau_{\text{reg}}^{(1)} &= 1 + \varepsilon - \varepsilon \log \frac{m_t^2}{4\pi\mu^2} - \varepsilon \gamma_E + \mathcal{O}(\varepsilon^2) \\ \rho_{\text{reg}}^{(2)} &= A \left(\frac{1}{\varepsilon} - 2 \log \frac{m_t^2}{4\pi\mu^2} - 2\gamma_E \right) + f_\rho(r) + \mathcal{O}(\varepsilon) \\ \tau_{\text{reg}}^{(2)} &= B \left(\frac{1}{\varepsilon} - 2 \log \frac{m_t^2}{4\pi\mu^2} - 2\gamma_E \right) + f_\tau(r) + \mathcal{O}(\varepsilon) \end{aligned} \quad (23)$$

as obtained from eqs. (18) and (22) and from the one-loop result up to $\mathcal{O}(\varepsilon)$.

Renormalization amounts to expressing g_t in terms of the physical quantities m_t and G_μ , related to g_t at the tree level by eq. (13). This relation must be corrected by one-loop effects. For this purpose we define m_t as the location of the pole of the top propagator $S_t(p)$ and G_μ as the charged-current Fermi constant measured in the μ decay. Defining, close to the pole,

$$S_t^{-1}(p) \simeq iZ_{2L}^t p_L + iZ_{5R}^t p_R + g_t v Z_m \quad (24)$$

one has

$$m_t = g_t v \frac{Z_m}{\sqrt{Z_{2L}^t Z_{2R}^t}}. \quad (25)$$

From the Ward identities (see Appendix A) one also has, for the W mass

$$M_W^2 = \frac{g^2 v^2}{2} Z_W^2, \quad (26)$$

where the g is the $SU(2)$ -gauge coupling constant, which is not renormalized by pure g_t^2 effects. Therefore

$$G_\mu = \frac{\sqrt{2}g_t^2}{8M_W^2} = \frac{\sqrt{2}}{4v^2 Z_3^2} \quad (27)$$

so that, from eqs. (25) and (27),

$$g_t^2 = 2\sqrt{2}G_\mu m_t^2 \frac{Z_3^2 Z_{2L}^t Z_{2R}^t}{Z_m^2}. \quad (28)$$

From the diagrams of Fig. 3 one has

$$\begin{aligned} Z_m &= 1 + \frac{g_t^2}{(4\pi)^2} \left[\frac{1}{2} - \frac{1}{2} \log r \right] \\ Z_{2L}^t &= 1 + \frac{g_t^2}{(4\pi)^2} \left[\frac{7}{8} + \frac{1}{4} \log r + \frac{1}{2} \left(\frac{1}{\varepsilon} - \gamma_E - \log \frac{m_t^2}{4\pi\mu^2} \right) \right] \\ Z_{2R}^t &= 1 + \frac{g_t^2}{(4\pi)^2} \left[\frac{15}{8} + \frac{1}{4} \log r + \frac{1}{\varepsilon} - \gamma_E - \log \frac{m_t^2}{4\pi\mu^2} \right] \end{aligned} \quad (29)$$

whereas Z_3^2 is given in eq. (13). The replacement of g_t^2 in eqs. (23) with eq. (28), and the various Z factors expanded up to order g_t^2 gives ρ and τ in terms of renormalized quantities, except for a finite residual contribution of order m_t^4 arising from the interplay of the $1/\varepsilon$ term in the renormalization constants and the $O(\varepsilon)$ terms in the one-loop regularized expressions $\rho_{\text{reg}}^{(1)}$, $\tau_{\text{reg}}^{(1)}$.

To obtain it, we must remember that the m_t^2 factor in the logarithms appearing in $\rho_{\text{reg}}^{(1)}$, $\tau_{\text{reg}}^{(1)}$ is actually $(g_t v)^2$. Therefore, according to eq. (25), it must be replaced by the combination

$$m_t^2 \frac{Z_{2L}^t Z_{2R}^t}{Z_m^2} \quad (30)$$

before the expansion in g_t^2 is made.

5 Results and conclusions

The overall asymptotic expressions for ρ and τ expanded up to second order in the variable

$$x = \frac{C_\mu m_t^2}{8\pi^2 \sqrt{2}},$$

so that

$$\frac{1}{\rho} - 1 = -N_c x (1 + x\rho^{(2)}) \quad (31)$$

and

$$\tau = -2x (1 + x\tau^{(2)}),$$

are:

(i) for $r = (m_t/m_H)^2 \ll 1$

$$\begin{aligned} \rho^{(2)} &= \frac{49}{4} + \pi^2 + \frac{27}{2} \log r + \frac{3}{2} \log^2 r + \\ &+ \frac{r}{2} (2 - 12\pi^2 + 12 \log r - 27 \log^2 r) + \\ &+ \frac{r^2}{48} (1613 - 240\pi^2 - 1500 \log r - 720 \log^2 r) + O(r^3) \end{aligned} \quad (32)$$

$$\begin{aligned} \tau^{(2)} &= \frac{1}{144} [311 + 24\pi^2 + 282 \log r + 90 \log^2 r + \\ &- 4r(40 + 6\pi^2 + 15 \log r + 18 \log^2 r) + \\ &+ \frac{3r^2}{100} (24209 - 6000\pi^2 - 45420 \log r - 18000 \log^2 r)] + O(r^3) \end{aligned}$$

where we have included some sub-asymptotic contributions to improve the convergence to the exact formula,⁵

(ii) for $r \gg 1$

$$\begin{aligned} \rho^{(2)} &= 19 - 2\pi^2 - \frac{4\pi}{\sqrt{r}} + O\left(\frac{\log r}{r}\right) \\ \tau^{(2)} &= \frac{27 - \pi^2}{3} + \frac{4\pi}{\sqrt{r}} + O\left(\frac{\log r}{r}\right) \end{aligned} \quad (33)$$

The $r \rightarrow \infty$ limit of eq. (34) confirms the result given in ref. [3]. These analytic expressions are not sufficient to allow an accurate calculation of the second-order coefficients $\rho^{(2)}$ and $\tau^{(2)}$ for $m_t \simeq m_H$. At the same time the full unexpanded analytic expressions are too long to be given explicitly. In table 1 we give the numerical values of $\rho^{(2)}$ and $\tau^{(2)}$ as functions of m_H/m_t . These numerical values are compared with the asymptotic expansions at low and large m_H/m_t in Fig. 5.

The knowledge of the second-order coefficients in the expansion of ρ and τ gives a way to judge the speed of convergence of the perturbative expansion itself. This is illustrated in Fig. 6, where we compare the first-order and second-order expressions for $\frac{1}{\rho} - 1$ and τ for different values of m_H in the $m_t = 150 - 300 \text{ GeV}$ interval. As is apparent from these figures, even for $m_t = 300 \text{ GeV}$ the speed of convergence is good for any reasonable value of the Higgs mass. This strengthens the significance of the upper bounds on the top mass that are obtained from the analyses of the electroweak precision data.

The numerical significance of these m_t^4 corrections for some of the electroweak precision observables currently measured at LEP is illustrated in Figs. 7, 8. In the ranges $m_t = 150 - 300 \text{ GeV}$ and $m_H = 50 - 2000 \text{ GeV}$ we show the Standard Model predictions for the Z leptonic width, $\Gamma(Z \rightarrow e^+ e^-)$, the forward-backward $e^+ e^- \rightarrow \mu^+ \mu^-$ asymmetry at the Z pole, A_{FB}^μ (both affected by ρ only) and the total Z width, Γ_Z (affected by ρ and τ). These graphs are obtained using the ZFITTER code [5], with the inclusion of the m_t^4

⁵The expression for $\tau^{(2)}$ appearing in eq. (17) of reference [4] contains a misprint.

corrections described in this paper. For comparison we also show the range of values that these same observables would obtain if we set to zero the second-order coefficients $\rho^{(2)}$ and $\tau^{(2)}$ for $m_H = 2 \text{ TeV}$, where the effect is larger.

Acknowledgements

We are grateful to Luciano Maiani for conversations that stimulated our interest in the calculation described in this paper and to Dmitri Bardin for providing us with several tables obtained with the ZFITTER code.

References

- [1] M. Veltman, *Nucl. Phys. B* **123** (1977) 89.
- [2] A. A. Akhundov, D. Yu. Bardin and T. Riemann, *Nucl. Phys. B* **276** (1988) 1;
F. Diakonos and W. Wetzel, preprint HD-THEP-88-21 (1988);
W. Beenakker and W. Hollik, *Z. Phys. C* **40** (1988) 141;
J. Bernabeu, A. Pich and A. Santamaria, *Phys. Lett. B* **200** (1988) 569;
J. Bernabeu, A. Pich and A. Santamaria, CERN preprint TH-5931/90 (Nov 1990);
B. Lynn and R. Stuart, *Phys. Lett. B* **252** (1990) 676.
- [3] J. Van der Bij and F. Hoogeveen, *Nucl. Phys. B* **283** (1987) 477.
- [4] R. Barbieri, M. Beccaria, P. Ciafaloni, G. Curci and A. Viceré
Phys. Lett. B **288** (1992) 95.
- [5] D. Bardin et al., CERN preprint TH-6443/92 (March 1992)
- [6] A. Cohen, H. Georgi and B. Grinstein, *Nucl. Phys. B* **232** (1984) 61;
M. Consoli, W. Hollik and F. Jegerlehner, *Phys. Lett. B* **227** (1989) 167;
H. Georgi, *Nucl. Phys. B* **363** (1991) 301.
- [7] W. Siegel (1980) *Phys. Lett. B* **94B** 37.
- [8] G. Altarelli, G. Curci, G. Martinelli and S. Petrarca *Nucl. Phys. B* **187** (1981) 461;
A.J. Buras, P.H. Weisz *Nucl. Phys. B* **187** (1990) 461;
B. Grinstein, R. Springer and M.B. Wise *Phys. Lett. B* **202** (1988) 138.
- [9] M. Beccaria, G. Curci and A. Viceré, in preparation

Appendix A

In this appendix we explain in some detail the Ward identities used to obtain the relations (8) in section 2.

Let us recall that our aim is to identify in the Standard Model Lagrangian terms contributing to $O(g_2^2)$, $O(g_2^4)$ effects. All the couplings involving more than one gauge fields are irrelevant in this limit and the gauge bosons can be seen as external fields coupled to the symmetry currents of the Lagrangian (1) through the following term

$$\Delta \mathcal{L} = -\frac{g}{c} (J_\mu^3 - s^2 J_\mu^{em}) Z_\mu - \frac{g}{\sqrt{2}} (J_\mu^+ W_\mu^- + J_\mu^- W_\mu^+) ; \quad (34)$$

J_μ^\pm , J_μ^3 stand for the $SU(2)$ currents and J_μ^{em} is the electromagnetic current, which is exactly conserved and does not renormalize.

By defining

$$J_\mu^3 = \frac{1}{2} [-\bar{t}_L \gamma_\mu t_L + \bar{b}_L \gamma_\mu b_L + i(\varphi^+ \partial_\mu \varphi^- - \varphi^- \partial_\mu \varphi^+) + (H \partial_\mu \chi - \chi \partial_\mu H)] , \quad (35)$$

the conserved current is given by

$$J_\mu^3 = \hat{J}_\mu + \frac{v}{\sqrt{2}} \partial_\mu \chi , \quad (36)$$

Analogously, for the charged current one has

$$J_\mu^+ = -\bar{b}_L \gamma_\mu t_L + \frac{1}{\sqrt{2}} (H \partial_\mu \varphi^+ - \varphi^+ \partial_\mu H) + \frac{i}{\sqrt{2}} (\chi \partial_\mu \varphi^+ - \varphi^+ \partial_\mu \chi) , \quad (37)$$

in terms of which the conserved current is

$$J_\mu^+ = \hat{J}_\mu^+ + v \partial_\mu \varphi^+ . \quad (38)$$

The conservation of the currents J_μ^3 , J_μ^\pm implies the existence of Ward identities relating different Green functions.

Let us first consider the ones relevant to the computation of the ρ parameter: in the language of the generating functional of 1PI Green functions Γ , and taking into account that tadpoles are set to zero by renormalization conditions, we easily derive that

$$\begin{aligned} \frac{\partial^x}{\partial Z_\mu} \frac{\delta \Gamma}{\delta Z_\mu(x) \delta Z_\nu(y)} &= -\frac{gv}{\sqrt{2}c} \frac{\delta \Gamma}{\delta \chi(x) \delta Z_\nu(y)} \\ \frac{\partial^x}{\partial Z_\mu} \frac{\delta \Gamma}{\delta Z_\mu(x) \delta \chi_\nu(y)} &= -\frac{gv}{\sqrt{2}c} \frac{\delta \Gamma}{\delta \chi(x) \delta \chi(y)} \end{aligned} \quad (39)$$

$$\begin{aligned} \frac{\partial^x}{\partial W_\mu^+} \frac{\delta \Gamma}{\delta W_\mu^+(x) \delta W_\nu^-(y)} &= \frac{igv}{\sqrt{2}} \frac{\delta \Gamma}{\delta \varphi^+(x) \delta W_\nu^-(y)} \\ \frac{\partial^x}{\partial W_\mu^+} \frac{\delta \Gamma}{\delta W_\mu^+(x) \delta \varphi^-(y)} &= \frac{igv}{\sqrt{2}} \frac{\delta \Gamma}{\delta \varphi^+(x) \delta \varphi^-(y)} , \end{aligned} \quad (40)$$

which combine to give:

$$\begin{aligned}\frac{\partial^x \partial_y^\nu}{\delta Z_\mu(x) \delta Z_\nu(y)} &= \frac{g^2 v^2}{2c^2} \frac{\delta \Gamma}{\delta \chi(x) \delta \chi(y)} \\ \frac{\partial^x \partial_y^\nu}{\delta W_\mu^+(x) \delta W_\nu^-(y)} &= \frac{g^2 v^2}{2} \frac{\delta \varphi^+(x) \delta \varphi^-(y)}{\delta \Gamma}.\end{aligned}\quad (41)$$

By going to momentum space and parametrizing the 1PI Green functions as follows:

$$\begin{aligned}\frac{\delta \Gamma}{\delta Z_\mu(q) \delta Z_\nu(-q)} \Big|_{q^2=0} &\simeq \frac{g^2 v^2}{2c^2} (Z-1) \delta_{\mu\nu} \\ \frac{\delta \Gamma}{\delta \chi(q) \delta \chi(-q)} &\simeq (Z_\chi^2 - 1) q^2 \text{ at } q^2 \simeq 0 \\ \frac{\delta \Gamma}{\delta W_\mu^+(q) \delta W_\nu^-(q)} \Big|_{q^2=0} &\simeq \frac{g^2 v^2}{2} (Z^\pm - 1) \delta_{\mu\nu} \\ \frac{\delta \Gamma}{\delta \varphi^+(q) \delta \varphi^-(q)} &\simeq (Z_\varphi^2 - 1) q^2 \text{ at } q^2 \simeq 0,\end{aligned}\quad (42)$$

one obtains

$$Z = Z_\chi^2, \quad Z^\pm = Z_\varphi^2, \quad (43)$$

and, in the limit $g_t \gg g$, for the vector boson masses

$$M_Z^2 = \frac{g^2 v^2}{2c^2} Z_\chi^2 \quad (44)$$

$$M_W^2 = \frac{g^2 v^2}{2} Z_\varphi^2.$$

The ρ parameter is therefore given by the ratio [6]

$$\rho = \frac{M_W^2}{M_Z^2 c^2} = \frac{Z_\varphi^2}{Z_\chi^2}. \quad (45)$$

Let us now consider the identity relevant to the decay $Z \rightarrow b\bar{b}$:

$$\begin{aligned}\frac{\partial^x}{\delta Z_\mu(x) \delta b(y) \delta \bar{b}(z)} &= -\frac{gv}{\sqrt{2c} \delta \chi(x) \delta b(y) \delta \bar{b}(z)} + \\ &+ \frac{ig}{c} \left[\frac{\delta \Gamma}{\delta b(x) \delta \bar{b}(z)} \left(\frac{1}{2} P_L - \frac{1}{3} s^2 \right) \delta(x-y) + \right. \\ &\quad \left. - \delta(x-z) \left(\frac{1}{2} P_R - \frac{1}{3} s^2 \right) \frac{\delta \Gamma}{\delta b(y) \delta \bar{b}(x)} \right].\end{aligned}\quad (46)$$

By going to momentum space and defining

$$\begin{aligned}\frac{\delta \Gamma}{\delta Z_\mu(p-p) \delta b(p) \delta \bar{b}(-p')} &= -\frac{ig}{2c} \left[\left(1 - \frac{2}{3} s^2 \right) Z_1 \gamma_\mu P_L - \frac{2}{3} s^2 \gamma_\mu P_R \right] \text{ at } p \simeq p' \\ \frac{\delta \Gamma}{\delta \chi(p-p) \delta b(p) \delta \bar{b}(-p')} &= Z_\chi^2 \frac{p' - p}{\sqrt{2} v} P_L \text{ at } p^2 \simeq 0 \\ \frac{\delta \Gamma}{\delta b(p) \delta \bar{b}(-p)} &= S_b^{-1}(p) = i Z_\varphi^2 p P_L + i \not{p} P_R \text{ at } p^2 \simeq 0\end{aligned}\quad (47)$$

one obtains

$$\begin{aligned}\frac{g}{2c} \left[\left(1 - \frac{2}{3} s^2 \right) Z_1 (p-p) P_L - \frac{2}{3} s^2 (p-p) P_R \right] = \\ -\frac{g}{2c} [Z_\chi^2 (p' - p) P_L] + \\ + \frac{g}{2c} \left[Z_2^b (p' - p) \left(1 - \frac{2}{3} s^2 \right) - \frac{2}{3} s^2 P_R \right]\end{aligned}\quad (48)$$

or

$$\left(1 - \frac{2}{3} s^2 \right) Z_1 = Z_\chi^2 + \left(1 - \frac{2}{3} s^2 \right) Z_2^b. \quad (49)$$

Taking into account the wave-function renormalization of b external lines and the absence, in the limit that we are considering, of the Z wave-function renormalization, one obtains for the physical $Z \rightarrow b\bar{b}$ vertex

$$V_\mu = -i \frac{g}{2c} \left[\left(1 - \frac{2}{3} s^2 + \frac{Z_\chi^2}{Z_2^b} \right) \gamma_\mu P_L - \frac{2}{3} s^2 \gamma_\mu P_R \right]. \quad (50)$$

Let us finally notice that the Ward identities (41) and (47) are valid also in the full Standard Model, if one works in the so called background field gauge, which ensures that the classical symmetries are preserved on the external lines, while in the internal (quantum) lines one has Slavnov Taylor identities.

Appendix B

In this appendix we address the question of regularization. In this work we have used the so called Naïve Dimensional Regularization scheme (NDR), which differs from the 't Hooft and Veltman (TV) dimensional scheme in the definition of γ_5 . The difference is sketched as follows:

NDR : anticommuting γ_5

$$\mathbf{TV} : \gamma_\mu = \gamma_\mu^T + \gamma_\mu^L; \quad [\gamma_\mu^T, \gamma_5] = 0; \quad \{\gamma_\mu^L, \gamma_5\} = 0,$$

The naïve scheme does not reproduce the Adler anomaly, as it gives a conserved axial current. As a counterpart, it is not internally consistent, since it is well known that the trace of a sufficiently high number of γ matrices does depend on the order of the operations [7]: this is related to the impossibility of defining a completely antisymmetric tensor in d dimensions.

In our calculation, however, we do not encounter any such ambiguity: for instance we never need to define a trace like $\text{Tr}[\gamma_5 \gamma_{\mu_1} \dots \gamma_{\mu_n}]$, nor the completely antisymmetric tensor. This means that the internal inconsistency of the NDR scheme does not manifest itself in our computation, which makes the use of the NDR scheme legitimate. This is essentially connected to the fact that we never compute the correlation function of three currents. Other examples of the possibility of utilizing NDR may be found for instance in [8].

The main advantage of the NDR scheme is that it is easier to use in practical calculations, and, even more so, it does not break the Ward identities we used in our work, so there

is no need of finite renormalizations other than the ones already described in section 4. By using an alternative renormalization scheme, such as the TV or the Bogolioubov-Parasiuk-Hepp-Zimmermann (BPHZ) ones, it is found that the Ward identities are in general broken and need to be reinforced by finite renormalizations: our statement is that the physical results are the same. A tedious calculation shows that, by working in a safe scheme, as the BPHZ one, it is possible at least up to two loops to choose finite renormalizations of the effective Lagrangian and the currents, which connect the physical results to the ones obtained in the naïve scheme. This detailed analysis will be published elsewhere [9].

| m_H/m_t | $\rho^{(2)}$ | $\tau^{(2)}$ |
|-----------|--------------|--------------|
| 0.1 | -1.82 | 4.67 |
| 0.2 | -2.70 | 3.90 |
| 0.3 | -3.46 | 3.30 |
| 0.4 | -4.13 | 2.83 |
| 0.5 | -4.72 | 2.46 |
| 0.6 | -5.25 | 2.16 |
| 0.7 | -5.74 | 1.92 |
| 0.8 | -6.18 | 1.73 |
| 0.9 | -6.58 | 1.59 |
| 1.0 | -6.95 | 1.47 |
| 1.1 | -7.30 | 1.38 |
| 1.2 | -7.62 | 1.32 |
| 1.3 | -7.91 | 1.27 |
| 1.4 | -8.19 | 1.24 |
| 1.5 | -8.44 | 1.23 |
| 1.6 | -8.68 | 1.23 |
| 1.7 | -8.90 | 1.24 |
| 1.8 | -9.11 | 1.26 |
| 1.9 | -9.30 | 1.29 |
| 2.0 | -9.48 | 1.33 |
| 2.1 | -9.66 | 1.37 |
| 2.2 | -9.81 | 1.42 |
| 2.3 | -9.96 | 1.47 |
| 2.4 | -10.1 | 1.53 |
| 2.5 | -10.2 | 1.60 |
| 2.6 | -10.4 | 1.66 |
| 2.7 | -10.5 | 1.73 |
| 2.8 | -10.6 | 1.80 |
| 2.9 | -10.7 | 1.87 |
| 3.0 | -10.8 | 1.95 |

Table 1: Values of $\rho^{(2)}$ and $\tau^{(2)}$ as functions of m_H/m_t

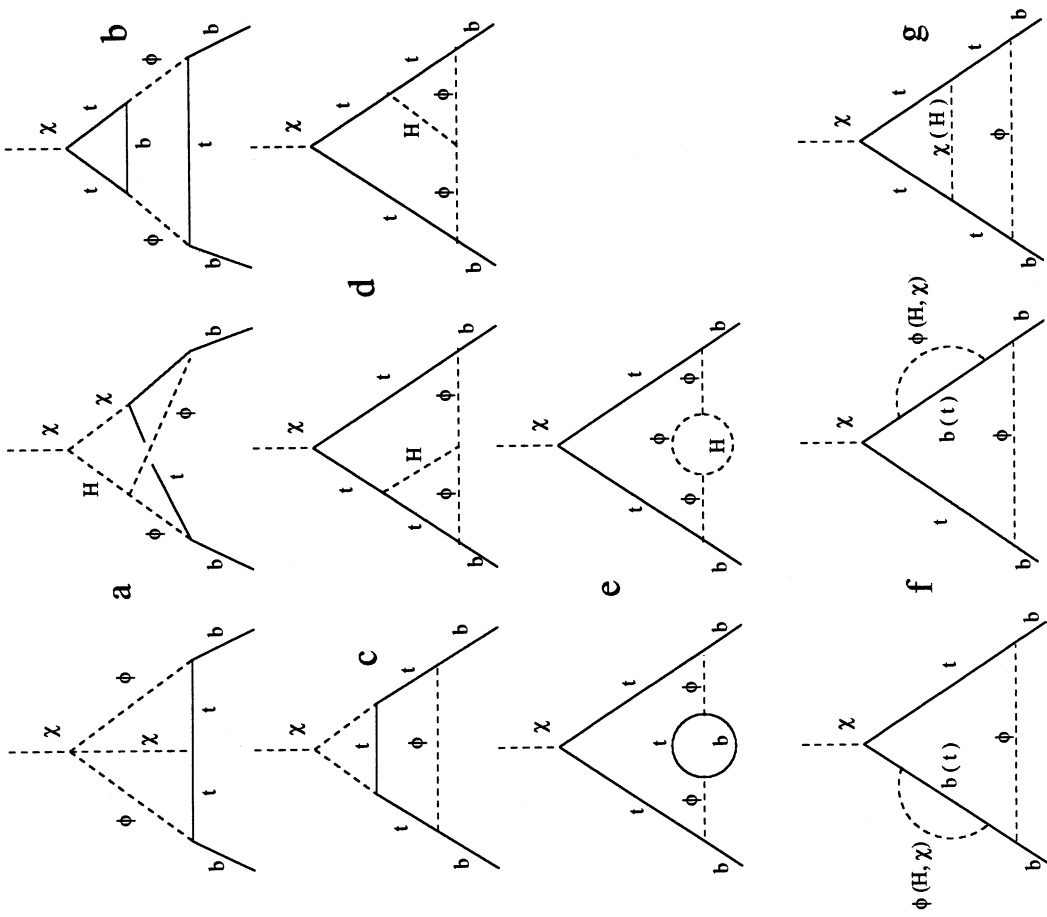


Figure 2: 2 Loop graphs contributing to Z_1^λ

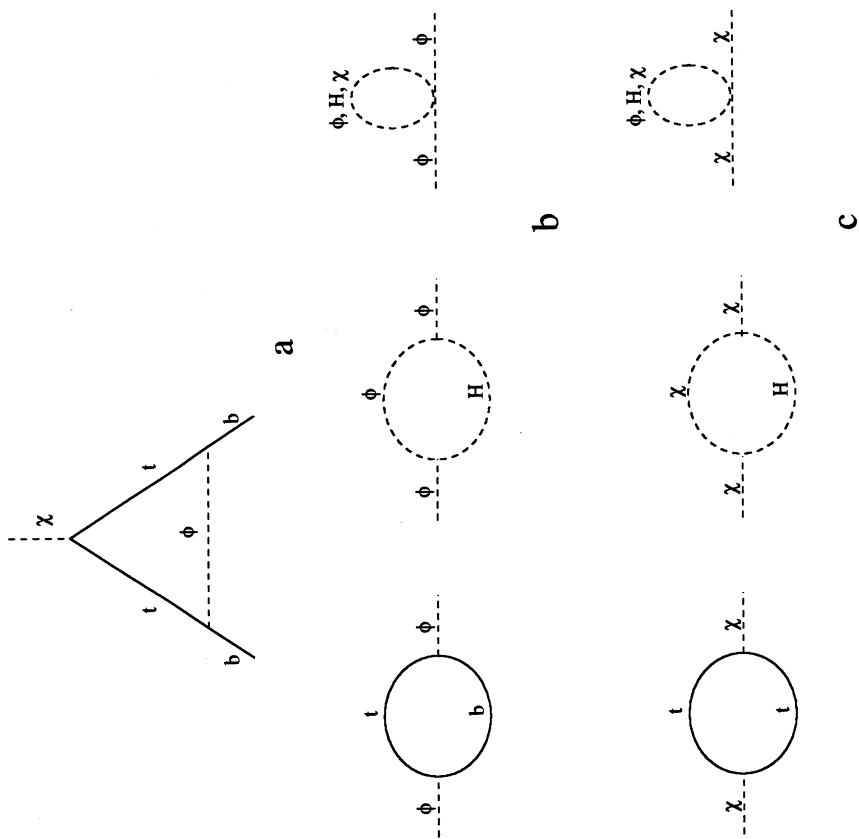


Figure 1: 1 Loop graphs contributing to ρ and τ

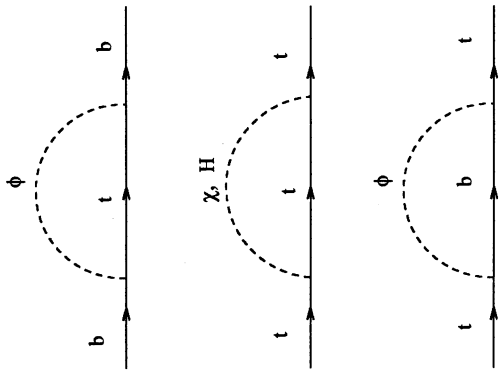


Figure 3: t and b quarks self energy

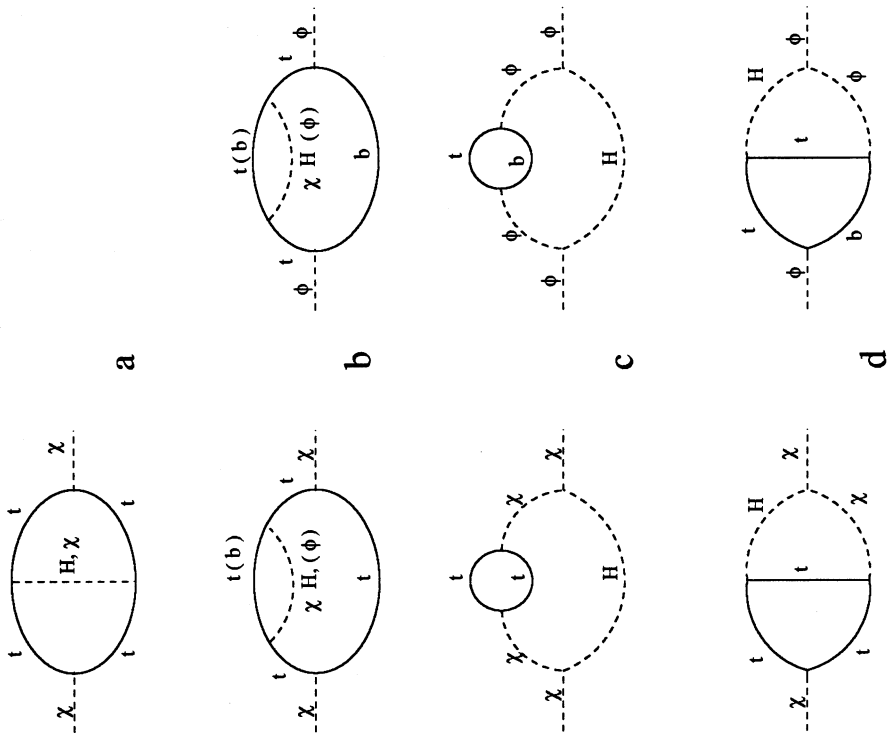


Figure 4: 2 Loop diagrams contributing to $Z_2^t - Z_2^b$

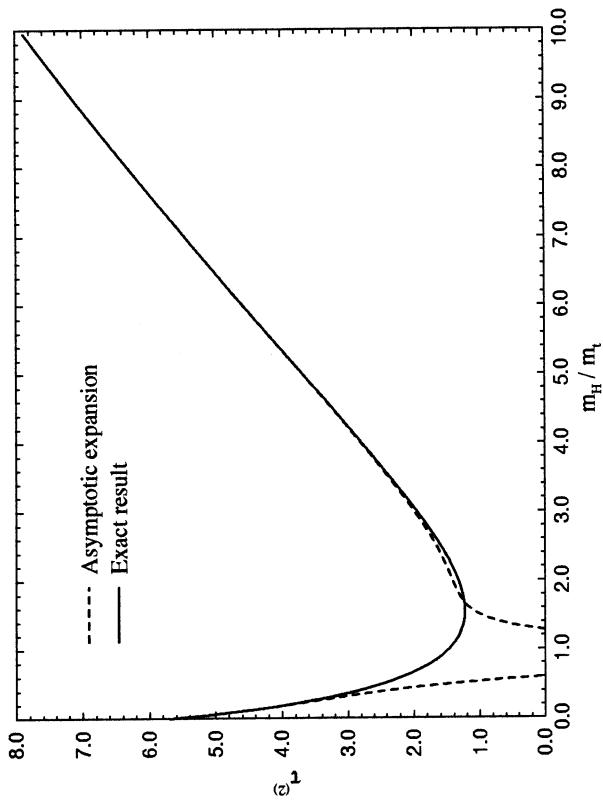
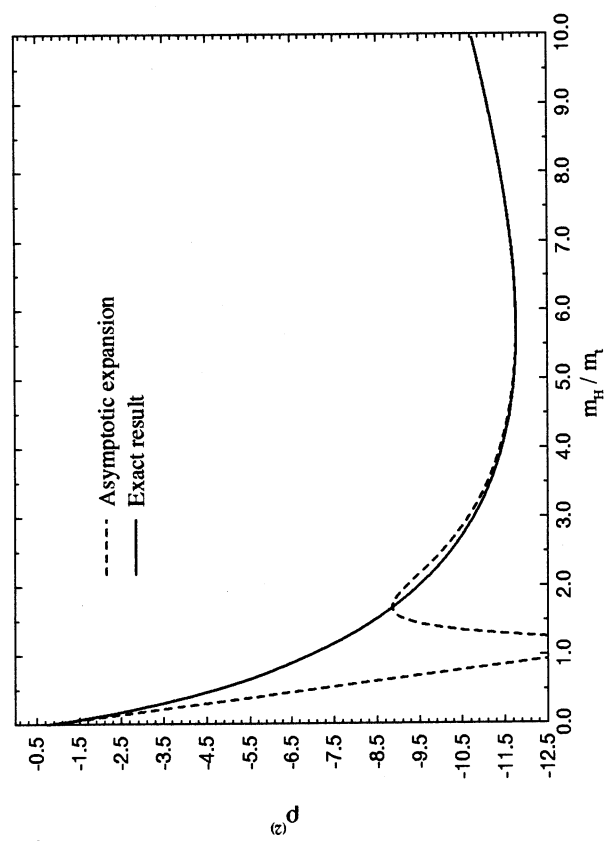
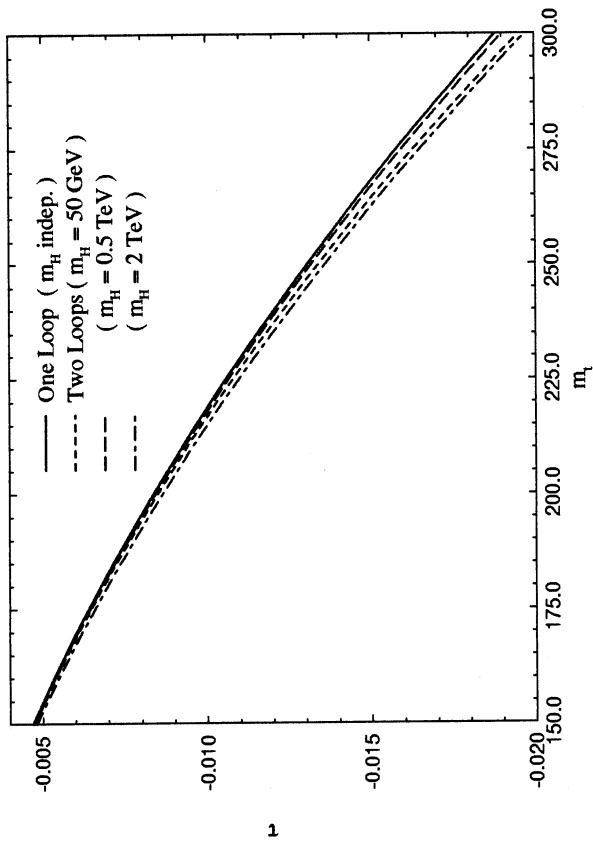
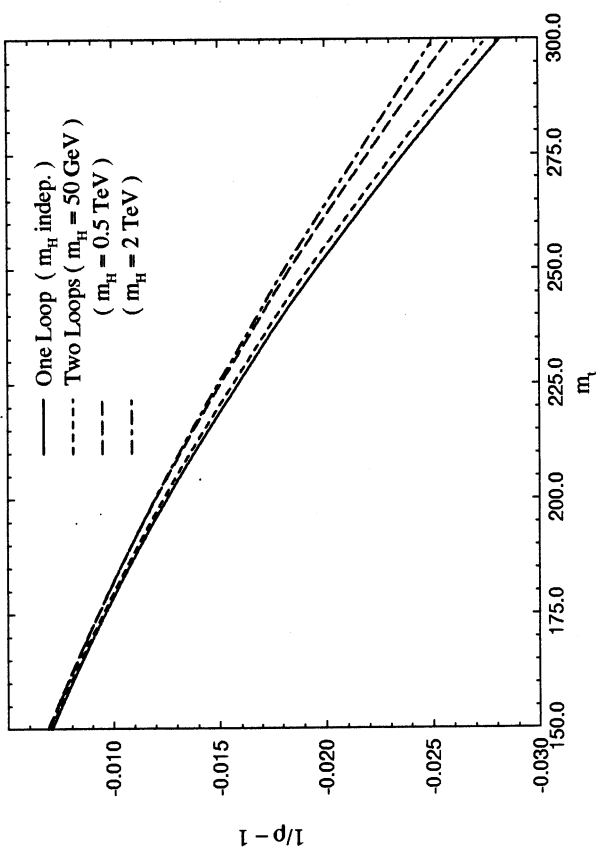


Figure 6: $\frac{1}{\rho} - 1$ and τ

Figure 5: $\rho^{(2)}$ and $\tau^{(2)}$

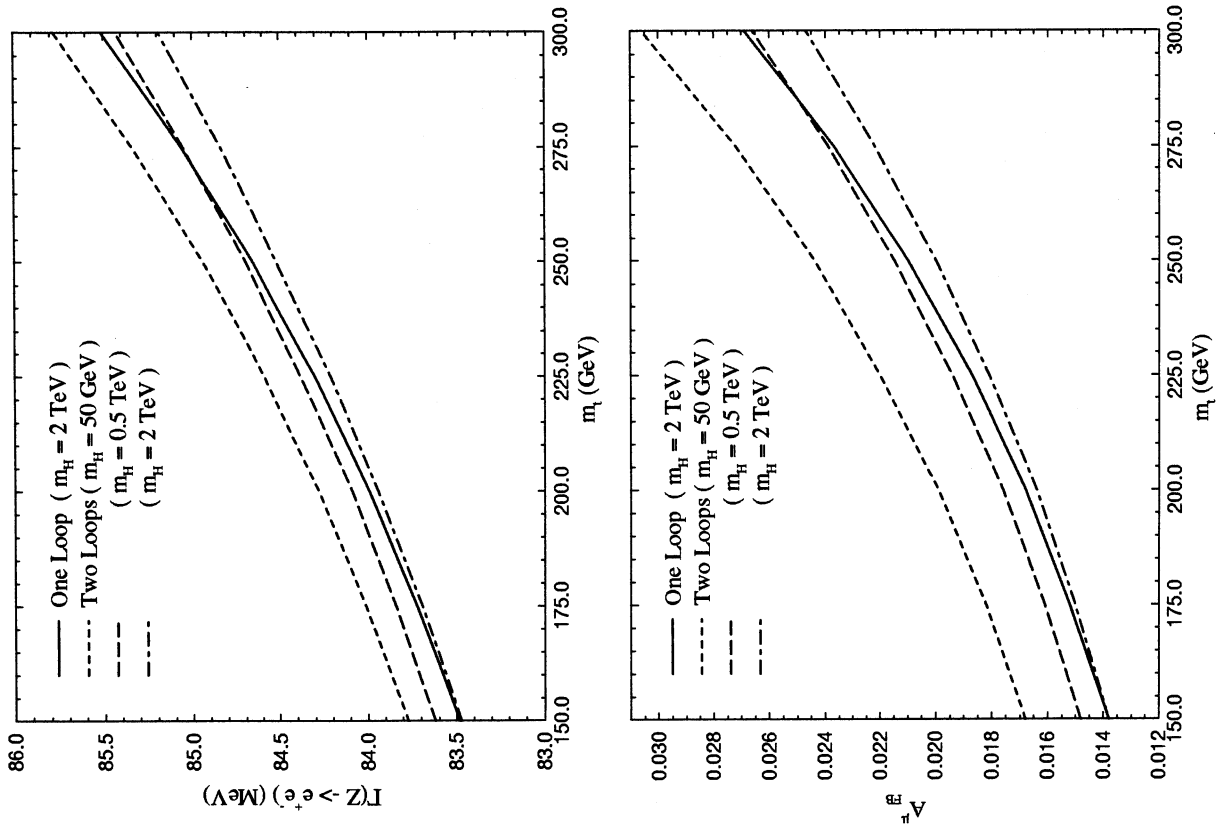


Figure 7: $\Gamma(Z \rightarrow e^+e^-)$, A_{FB}^e (ZFITTER code)

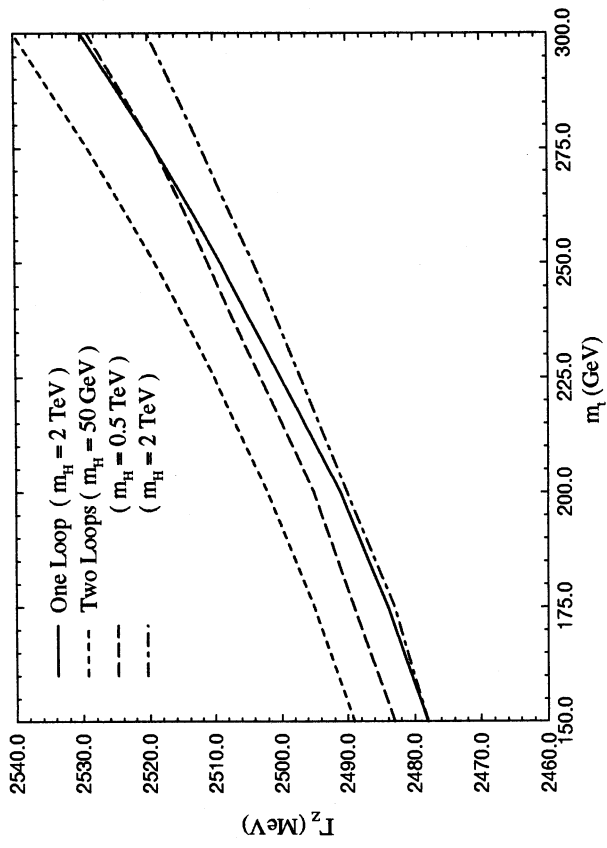


Figure 8: Γ_Z^e (ZFITTER code)